# Analysis of Building Destruction as a Consequence of Military Actions Based on Multi-Temporal Remote Sensing Data – A Case Study in Moschum and Mariupol Cities, Ukraine

**Chetverikov, B.,[1*] Trevoho, I.,[2] Prokhorchuk, O.,[3] Vladimirov, S.[4] and Kilaru, V.[5]**
[1]Department of Photogrammetry and Geoinformatics, Lviv Polytechnic National University, Lviv, Ukraine, 12, S.Bandery str., E-mail: borys.v.chetverikov@lpnu.ua*
[2]Department of Geodesy, Lviv Polytechnic National University, Lviv, Ukraine, 12, S.Bandery str., E-mail: itrevoho@gmail.com
[3]Ukrainian Aerial Geodesic Association (UAGA), Kyiv, Ukraine, 77, Sichovyh Striltsiv str., E-mail: vaga.aero@gmail.com
[4]Kaylas-K LLC., Khmelnytskyy, Ukraine, 5, Haharina Str., +38067491-43-04 E-mail: kaylas3000sv@gmail.com
[5]Public Union "Ukrainian Society of Geodesy and Carography", Honorary Surveyor of Ukraine, Chernivtsi, Ukraine, E-mail: cheytverikov@email.ua
**Corresponding Author*

**DOI: https://doi.org/10.52939/ijg.v21i5.4157**

**Abstract**
*The article presents a methodology for analyzing the destruction of buildings caused by Russian military aggression against Ukraine based on multi-temporal remote sensing (RS) data. The study aims to assess the scale of destruction using satellite imagery, geoinformation technologies, and automated data processing algorithms. The research consists of two analytical case studies. The first case examines the destruction of buildings in Moshchun (Kyiv region) by comparing satellite images taken before and after the full-scale invasion. To improve the accuracy of damage assessment, the analysis results were verified using aerial imagery obtained after the de-occupation of the area. It was determined that the number of destroyed or damaged buildings in the village due to hostilities amounted to 663, of which 590 were completely destroyed. The second case focuses on determining the extent of building destruction in Mariupol by comparing multi-temporal satellite images with vector building layers that reflect the state of urban development before the onset of hostilities. The analysis was conducted using image processing algorithms and geospatial analysis implemented in the Python environment. It was established that during the full-scale invasion, 8,349 buildings were destroyed, including 2,013 multi-story buildings, of which 934 were completely demolished.*

**Keywords:** Building Destruction, Case Studies, Military Conflict, Multi-Temporal Analysis Remote Sensing

## 1. Introduction

Successful operation of many orbital systems conducting space surveying in various ranges of the electromagnetic spectrum allows for continuous monitoring of processes occurring on the Earth's surface. Timely detection of changes is one of the most important tasks of this observation. In a number of tasks related to the observation of specific objects from satellites, there is a need to analyze their dynamics. Especially often, such tasks arise during the study of various objects of human activity and the analysis of their impact on the environment. Sometimes this effect can be so imperceptible that it becomes possible to detect changes only after a long visual analysis of the images. In order to reduce the complexity of such work and to reduce the number of omissions of changed areas, special image processing algorithms are needed, which allow the selection of change areas in relation to image sequences [1]. The primary challenges in detecting differences (areas of change) in satellite images of the same region taken at different times are mainly due to varying survey conditions, which can result in differences between the images.

These differences may include variations in spatial resolution (due to the use of different devices or scanning angles), color characteristics (due to different devices or lighting conditions), slight discrepancies in referencing (due to surveys from different spacecraft), changes in perspectives (due to different surveying angles), and differences in shadows (due to the Sun's position). Change Detection, which involves identifying areas of change in multiple images of the same area, is used to monitor and analyze spatial changes over time. This process aims to detect new objects, determine the disappearance of objects, and analyze the changes in objects over time [2] and [3].

On February 24, 2022 Russian Federation started a new stage of the eight-year war against Ukraine a full-scale offensive. The enemy carries out massive shelling and bombing of peaceful Ukrainian cities and villages. The Cabinet of Ministers made changes to the Procedures for the execution of urgent works related to the damage to buildings and structures and the determination of damage and losses caused to Ukraine as a result of the armed aggression of the Russian Federation. The relevant resolution project was adopted at the Government's regular meeting on June 14, leading to proposed changes that include recording damage caused by the Russian Federation's armed aggression to buildings and structures of both private, communal, and state ownership, conducting inspections of damaged objects through authorized bodies via commission or technical inspections, specifying the areas where damage and losses to housing funds, housing and communal services, and public buildings are recognized, and establishing the form and content of the commission examination report.

The aim of the work is to analyze building destruction as a consequence of military actions based on multi-temporal remote sensing data in order to assess the scale of damage and its impact on urban infrastructure in the village of Moschun and the city of Mariupol, Ukraine. The study is focused on identifying changes in building structures before and after military actions through the use of modern satellite image processing methods and geoinformation systems. The work involves conducting a comparative analysis of building conditions over different time periods, which makes it possible to identify areas of maximum destruction, determine the extent of damage to objects, and assess the dynamics of changes in the urban environment. The research results can be used for planning recovery measures, optimizing urban management, and supporting humanitarian programs aimed at restoring residential infrastructure.

It should be noted that the problem of obtaining differential indicators from space images or aerial photography data with the help of semi-automatic modules or programs was dealt with by many scientists both from Ukraine and abroad [4] and [5]. Among Ukrainian scientists who were engaged in obtaining differential indicators based on the Remote Sensing data, the topic of destruction due to natural disasters or cataclysms was considered mainly [6] and [7]. Among the latest studies of foreign scientists regarding differential indicators, the main attention is also paid to the change of forest cover, rivers, etc. [8] and [9]. Among the scientific works on this topic of the last decade, it is necessary to note the works [10] and [11], which consider the methods of automatic selection of contours of buildings on space images of high spatial resolution. Also, the algorithms for highlighting buildings on space images are described in the works of groups of authors [12][13][14][15] and [16]. Methods of object selection in space images using machine vision and artificial intelligence are discussed in articles [17] and [18]. The technology of applying semantic segmentation methods for the selection of objects on space images is considered in works [19] and [20].

The methodology of remote sensing change detection and monitoring has been widely reported in the research presented in [21]. The present review has assorted the detection approaches and drawn many useful conclusions. Based on the former classification methods, this article classifies change detection methods from its essence into seven groups, including direct comparison, classification, object-oriented method, model method, time-series analysis, visual analysis and hybrid methods. Authors discuss the effect and methods of geometric correction and radiometric correction in pre-processing. Relating to accuracy assessment, this paper summarize the present methods of exterior and interior check and emphasis on that how to get the ground truth.

The challenges that the change detection is currently facing and possible counter measures are also discussed. An automated method of measuring destruction in high-resolution satellite images is introduced in [22], where the authors apply deep-learning techniques combined with label augmentation and spatial and temporal smoothing to leverage the spatial and temporal structure of destruction. As a proof of concept, they apply this method to the Syrian civil war and reconstruct the evolution of damage in major cities across the country.

This approach allows generating destruction data with unprecedented scope, resolution, and frequency and makes use of the ever-higher frequency at which satellite imagery becomes available. A timely review of remote sensing applications for monitoring war-related environmental impacts is presented in [23], reflecting the rapidly growing number of publications in recent years. The paper's main objective is to locate the papers and find geographic link, sensor use, and environmental degradation type. Following a discussion of remote sensing's capabilities, this overview illustrates numerous environmental damages caused by military operations in various world places. This study found that wars have a detrimental influence on the ecosystem across the world, with major reasons being forest loss, oil spills, and urban growth. According to the findings, remote sensing, particularly middle-resolution satellite images, is extensively and successfully employed for environmental security monitoring.

An analysis of how geospatial technology could have been applied to reduce the impact of the Ammonium Nitrate explosion in Beirut is provided in [24]. Firstly, the disaster impacts on the build-up area were demarcated using Google Earth-based survey, Remote Sensing, and ArcGIS applications. According to the analysis, it was identified that the Ammonium Nitrate detonation incident in the Beirut port has extensively damaged the built-up area within a 2 km buffer zone from the explosion. Among them, fully demolished constructions are bounded to a 1 km buffer area while partially damage and less damage to buildings were encompassed within 5 km from the epicenter of the incident. The Quantity Distance Mapping Tool results depicted more as similar results to the results obtained through the aforementioned geospatial techniques in post-disaster impact analysis. Therefore, proper planning to locate built-up areas considering vulnerable places away from the possible disaster-induced location utilizing spatial techniques like Quantity Distance Mapping Tool would be more effective in pre-disaster preparedness as we all live in a hidden catastrophic environment. Thus, lessons learned from this Ammonium Nitrate detonation incident of the Beirut city, especially the importance of risk assessment and adherence to precaution measures are needed in any chemical operation sites as well as chemical storing sites. Taking into account all of the above, it is necessary to find effective operational methods of calculating the damage and destruction caused by Russian aggression. Our proposed method of determining destruction based on multi-temporal space images is quite inexpensive in terms of time and money [25][26] and [27].

## 2. Study Area

In this study, we examine two research sites, namely: the village of Moshchun (Figure 1(a)) in the Kyiv region and the city of Mariupol (Figure 1(b)). The first site was occupied by Russian forces in 2022 and suffered significant infrastructure destruction. The second research site is the city of Mariupol, which has been under Russian occupation since 2022 and remains so to this day. The majority of the city's buildings were destroyed during the hostilities, especially multi-story residential buildings, which are beyond restoration.

The village of Moshchun is located in the Kyiv region, in the Bucha district, approximately 20 km northwest of the center of Kyiv. It is situated near the Irpin River, which serves as a natural boundary between Kyiv and its northern suburbs. Before Russia's full-scale invasion of Ukraine in 2022, Moshchun had an official population of about 850 people, though the actual number of residents was around 2,000, including those with Kyiv registration. The area surrounding Moshchun is predominantly flat with slight elevations. The village is located within the Polissia Lowland, which is characterized by sandy soils, marshy areas, and significant forest cover. Sandy and sandy-loam soils with low fertility dominate the region, which is typical for Polissia. The primary natural landscapes consist of mixed forests, including pine, oak, birch, and alder trees. A significant portion of the area is covered by forests, contributing to its recreational potential. Near Moshchun, there are large forested areas that are part of the Kyiv Polissia ecosystem. This territory is rich in rare species of flora and fauna typical of mixed forests.

Mariupol is a port city located in southeastern Ukraine, in the Donetsk region, on the coast of the Azov Sea. It is situated approximately 100 km south of Donetsk and serves as an important industrial and transportation hub of the region. Before Russia's full-scale invasion of Ukraine in 2022, Mariupol had a population of about 430,000 people. However, due to hostilities, massive destruction, and a humanitarian catastrophe, the majority of residents were forced to leave the city. Mariupol is located within the Azov Upland, which gradually slopes down to the coast of the Azov Sea. The city's terrain is undulating, with elevation changes forming ravines and gullies, especially in the northern part. The natural vegetation is represented by steppe ecosystems, although significant areas are occupied by urban greenery, parks, and tree plantations, including acacia, poplar, and chestnut trees.

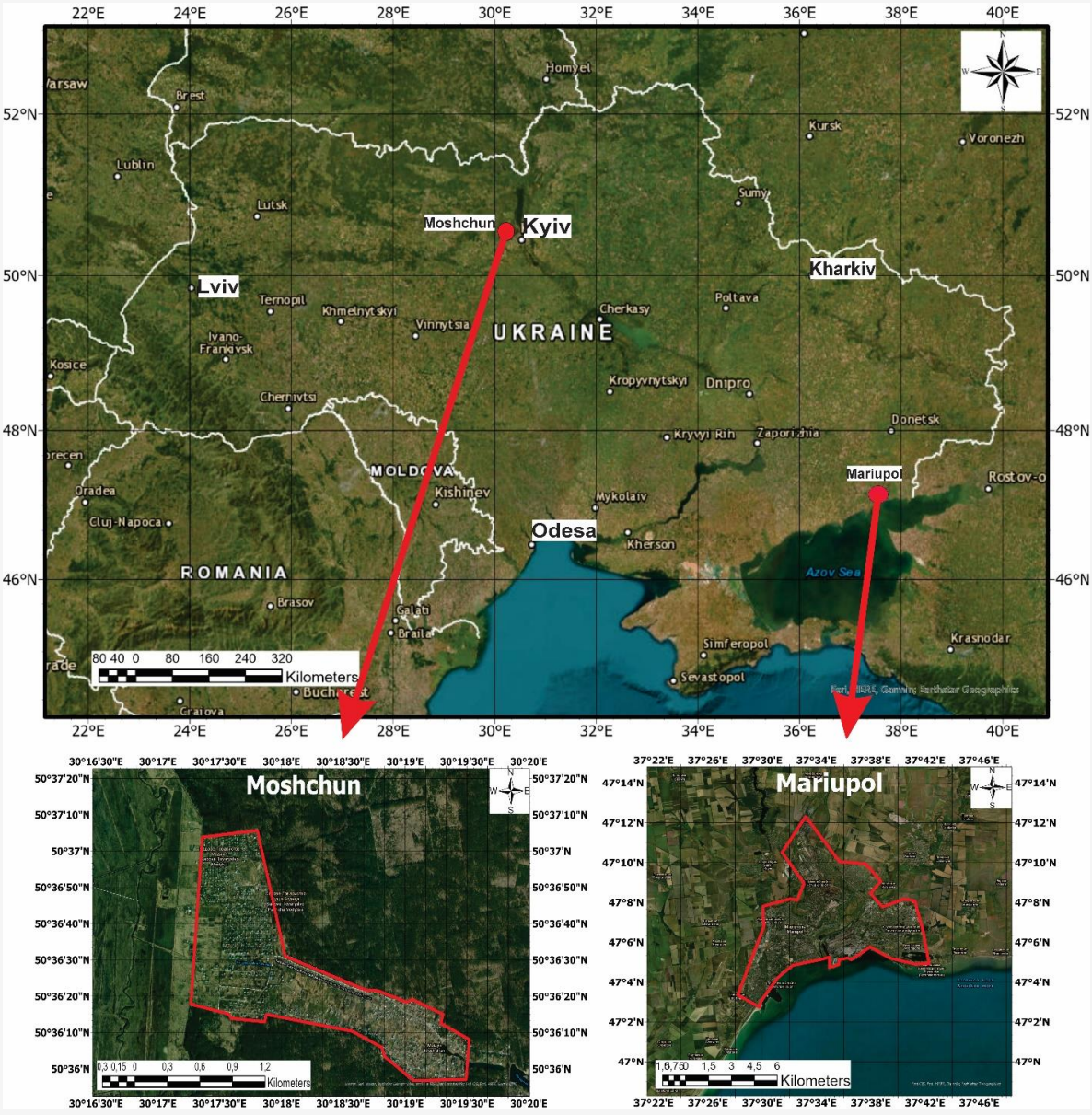


(a) (b)

Figure 1: Schematic location of the two research sites:
(a) the village of Moshchun; (b) the city of Mariupol

Until 2022, Mariupol was one of Ukraine's largest industrial centers, which had a significant impact on the local environment. The main sources of pollution were metallurgical plants, particularly Azovstal and the Ilyich Iron and Steel Works.

## 3. Materials and Methods

*3.1 Methodology for Detecting Building Destruction in Moshchun Village, Kyiv Region*

The purpose of the conducted research is to analyze the destruction of the infrastructure of the village of Moshchun as a result of the Russian occupation based on multi-temporal space images using a semi-automatic method in the DeltaCue module of the Erdas Imagine program. The object of our research in this paper is the infrastructure of the village of Moshchun near Kyiv, which was destroyed as a result of the partial occupation by the Russian Federation of the Kyiv region in the spring of 2022. The count of destroyed buildings was carried out based on space images from different times.

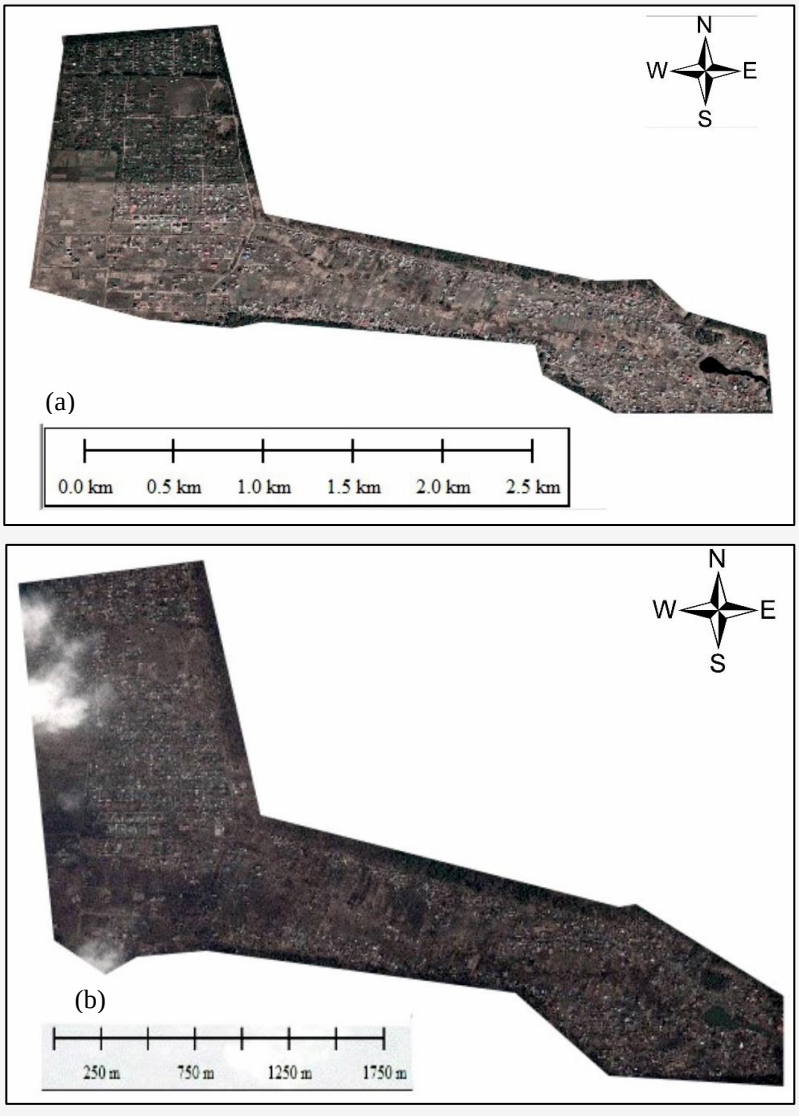


**Figure 2:** Maxar space satellite imagery: (a) 27/04/2020 (b) 11/05/2022

The input data for the research were: a space image of the territory of the Moshchun village near Kyiv, obtained in 27.04.2020 from Maxar space satellites (Figure 2(a)); space image obtained from Maxar satellites in 11.05.2022, after the partial occupation of Kyiv region (Figure 2(b)). Both images had a spatial resolution 0.3 m, and were saved in GeoTIFF format and transformed into the Latitude/Longitude-WGS84 projection and coordinate system. The implementation of the semi-automatic determination method of the destruction of buildings was carried out in the DeltaCue module. Unlike many other similar programs, which use only the raster subtraction function to obtain the difference index (namely, based on the geometric characteristics of objects), the DeltaCue module performs filtering according to three possible filters: spectral segmentation; incorrect registration of pixels of a pair of images; spatial filtering. The Imagine DeltaCue change detection module, operating in the ERDAS Imagine environment, is designed to significantly reduce the volume and complexity of work on the analysis of multi-temporal space images and is able to satisfy the requirements of both a novice and an experienced expert in the field of data processing.

Data processing and analysis in ERDAS Imagine DeltaCue is structured as projects that follow a specific sequence of steps, including preliminary processing, change detection, filtering of detected changes, and the display and analysis of those changes.

Automated pre-processing procedures, combined powerful algorithms for evaluating changes, flexible tool settings aimed at highlighting objects of interest - all this makes the ERDAS Imagine DeltaCue module an important link in the chain of Remote Sensing data processing. A set of customizable ERDAS Imagine DeltaCue data preprocessing procedures provides the ability to search for areas of change both throughout the image field and at well-defined points in space for more detailed analysis.

The interface of the special viewer of work results in this module - Change Viewer, is built in such a way that the user can analyze changes based on snapshots from different times with the involvement of additional data in various formats, as well as save the analysis results directly to the geodata base. ERDAS Imagine DeltaCue simplifies the process of detecting changes in multi-temporal images and gives the user the ability to quickly move from image to information. In addition, the selection of data for conversion into a shapefile can be precisely controlled by analyzing the data before and after comparison, as well as by examining the transition pixels. The primary features of the module's workflow can be outlined as follows. The process is structured as a step-by-step "wizard," which facilitates the configuration of processing parameters and the definition of the area of interest within the image. All settings related to the processing workflow, image parameters, and algorithm configurations are stored within the project file. The algorithms used for change detection include difference magnitude calculation, Tasseled Cap transformation, RGB color space transformation, and single-channel image analysis. The threshold values for change detection can be adjusted manually or automatically calculated by the system, optimizing processing time while allowing for operator intervention when necessary [28][29] and [30].

ERDAS Imagine DeltaCue incorporates a range of filters for refining the results of change detection, including spectral filters, spatial filters, and filters based on object types. Additionally, a specialized filter has been designed to minimize classification errors resulting from the misalignment of overlapping images. During the module's operation, automatic normalization of radiometric characteristics is performed to mitigate the impact of cloud cover and shadows. The integrated viewer within the DeltaCue interface provides geographically linked zones for simultaneous visualization of multi-temporal data. Furthermore, ERDAS Imagine DeltaCue enables the export of processed image data in the ESRI shapefile format.

To display changes, the following methods are used for data packets:

The image subtraction is defined in Equation 1:

$$R = A - B_A \quad \text{Equation 1}$$

Where: $A$ original image, $R$ is the result, is the original image (against which changes are detected), $B_A$ is the image with changes

The image division is defined in Equation 2

$$R = \frac{A}{B_A} \quad \text{Equation 2}$$

Principal Components is defined in Equation 3:

$$R = PC_{2A}\,(A - S_A) + PC_{2B}\,(B_A - S_B A) \quad \text{Equation 3}$$

Where: $A$ original image, $PC_{2A}$ is the second principal component multiplier for image A, $PC_{2B}$ is the second principal component multiplier for $B_A$, $S_A$ is the mean brightness of $A$, $S_B$ is the mean brightness of $B_A$.

The next step after data transformation involves classifying the Borodyansky district image using the OpenCV computer vision library, which is divided into three main stages: image recognition, visualization, and export of results. To configure decision trees and validate the obtained results, information about damaged areas is necessary. For this purpose, pixel-wise operations are performed. The next step involves image recognition through its classification using an ensemble of decision trees. Further, image post-processing is carried out. Mathematical morphology operations are used to correctly recognize adjacent pixels of damaged areas [31][32][33] and [34].

### *3.2 Methodology for Detecting Building Destruction in Mariupol*

Figure 3 presents the technological scheme for analyzing building destruction in the city of Mariupol based on multi-temporal satellite images and OpenStreetMap data. As input data, synthesized multi-temporal high-resolution satellite images of the city of Mariupol in RGB mode from Maxar satellites were obtained using the online service SASPlanet. Satellite images were acquired in 2020 and 2022, before and after the full-scale invasion (Figure 4).

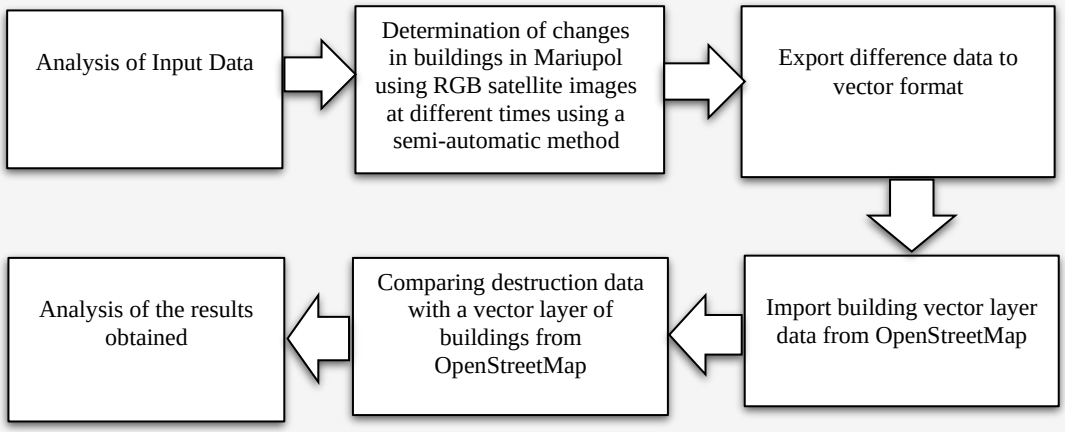


**Figure 3:** Technological diagram of the analysis of building destructions in the city of Mariupol based on multi-temporal satellite images and OpenStreet Map data

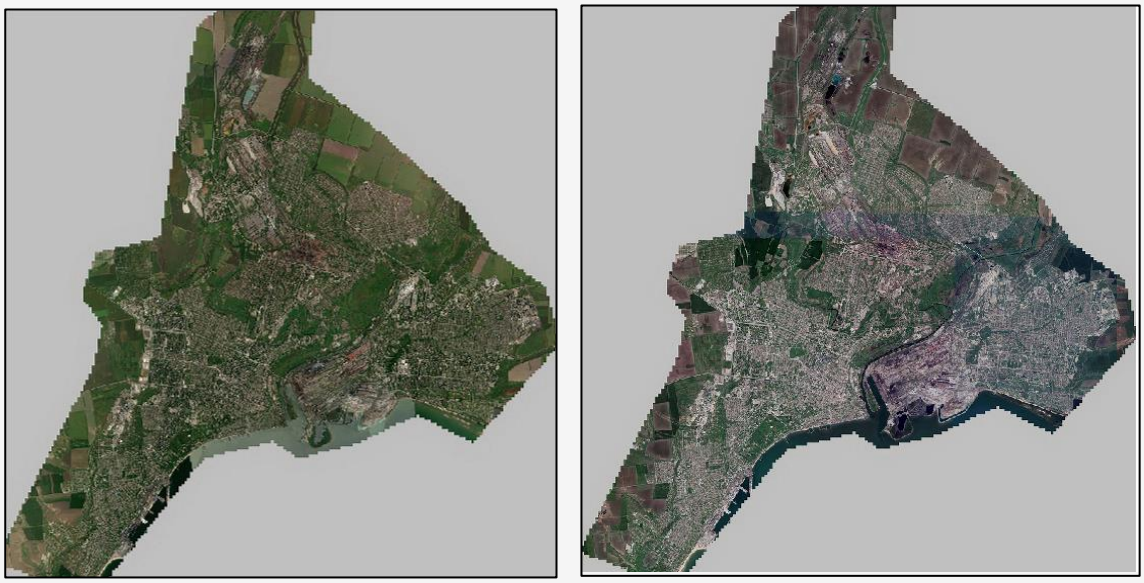

(a) (b)

**Figure 4:** RGB satellite images of the city of Mariupol, acquired from the Maxar satellite: (a) 2020; (b) 2022

The use of different data sources is due to the fact that Moshchun was de-occupied in 2022, which allowed for UAV aerial imaging and a visual assessment of the accuracy of the conducted research. In contrast, the destruction in Mariupol was studied solely through remote sensing, as the city remains under occupation, making physical access impossible. Since Mariupol is significantly larger than Moshchun, OSM data was used to obtain information on buildings before the destruction, simplifying the process of calculating the percentage of damage. The next step, for further comparison of the obtained data, was the need for reference information in the form of a vector layer of buildings before the full-scale invasion, that is, before the destructions.

For this, we used the Open Street Map (OSM) service (Figure 5). The data processing demonstrated was carried out using QGIS software. This open-source software has extensive functionality and is free of charge.

The building layer overlaid on the satellite imagery of Mariupol city in 2022 displays in Figure 6. After preparing all the input data, we analyzed the satellite images in 2020 and 2022 using the Change Detection module. As a result of these actions, a raster layer was obtained with difference indicators for all objects between the two satellite images, which also contained some false noise [35]. For convenience in further processing of these data, the objects were saved in a vector shapefile.

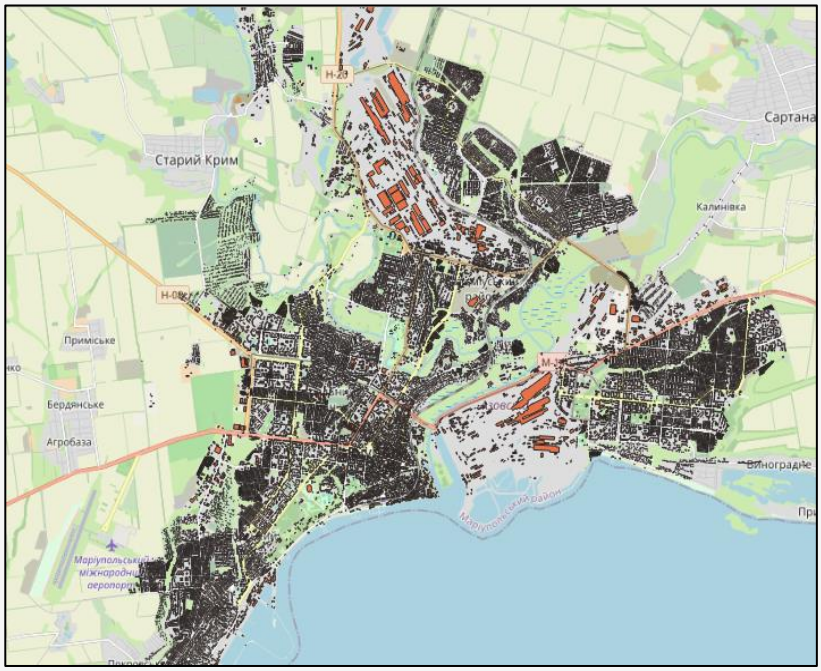


**Figure 5:** Vector layer of all buildings in the city of Mariupol before the full-scale invasion

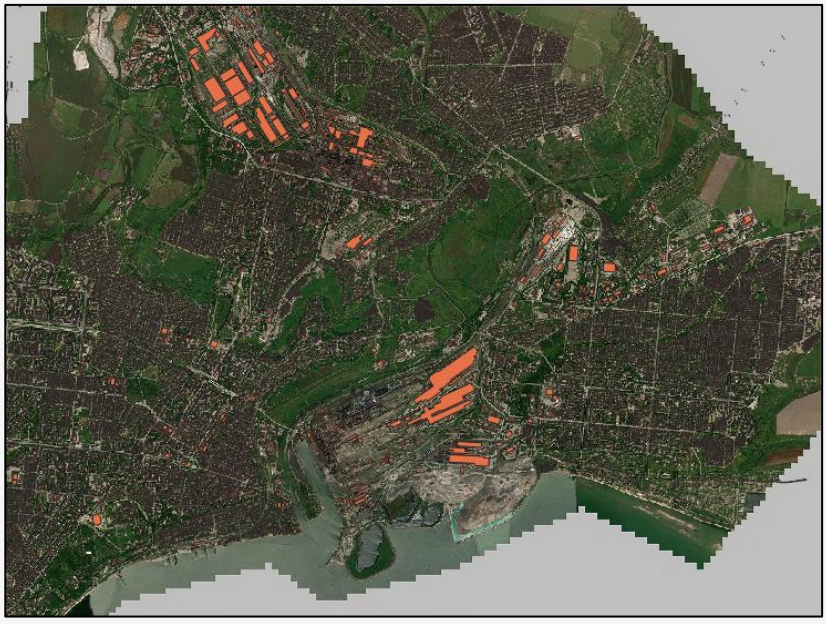

**Figure 6:** Vector layer of all buildings in the city of Mariupol on the 2022 satellite image

After that, the objects were classified by the field in the database 'type' into 18 classes, which were colored differently, with a total of 27,489,328 objects. By overlaying this data on the satellite image, we determined which color belonged to the building class, and all other objects were deleted. In this way, we obtained a vector layer with the building destructions caused by Russian aggression in 2022. Figure 7(a) shows the separate vector layer of building destructions obtained from multi-temporal satellite images, while Figure 7(b) shows the vector layer of destructions overlaid on the satellite image of Mariupol as of 2022.

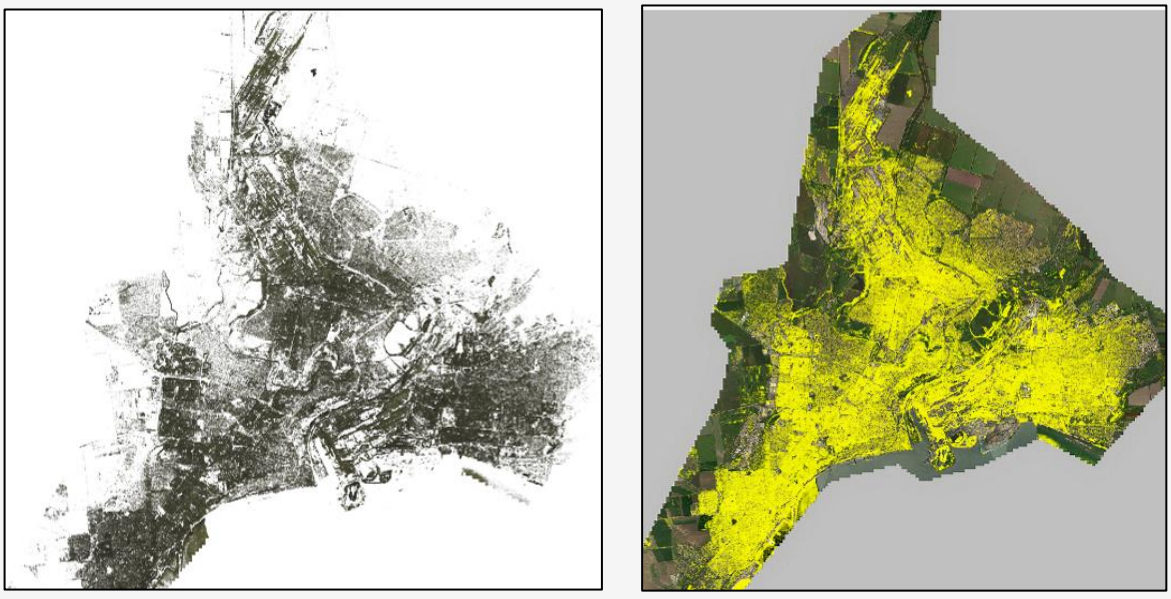

(a) (b)

**Figure 7:** Vector layer of building destructions as a result of Russian aggression, obtained from multi-temporal satellite images: (a) separate vector layer of building destructions obtained from multi-temporal satellite images; (b) vector layer of destructions overlaid on the satellite image of Mariupol as of 2022

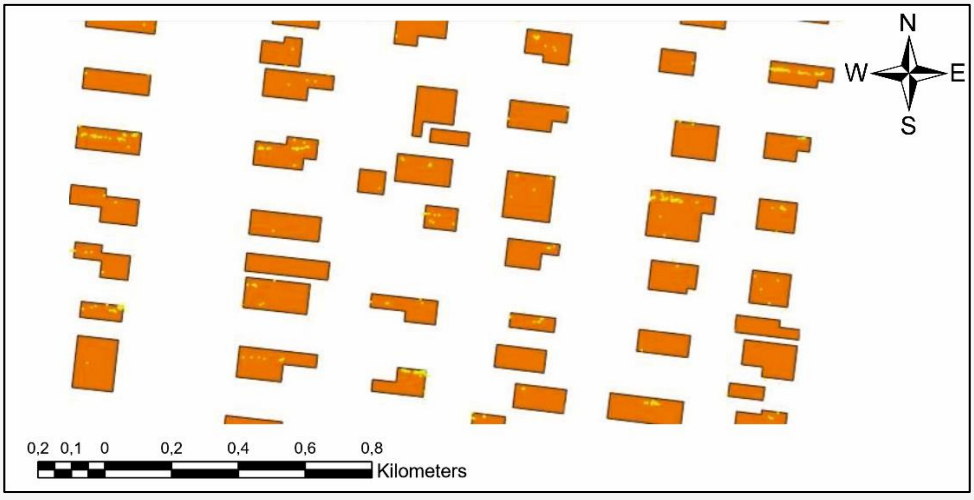


**Figure 8:** Vector layer of building destructions as a result of Russian aggression, overlaid on the building data from OSM

After filtering the difference indicators, there were still many vector objects located outside the building areas according to the OSM data. Initially, we perceived this as an error, but upon closer inspection of these data on the 2022 satellite image, it became clear that these objects represented the actual destructions of high-rise buildings.

Figure 8 shows an enlarged fragment of the city's private sector with the vector layer of buildings from OSM before the full-scale invasion and the vector layer of destructions. As seen in the figure, multiple difference indicator objects correspond to each house, which indicates partial destructions across the entire built-up area. Since multiple destruction objects correspond to each building, their total number does not match the total number of buildings. The task was set to create an additional script in PyQGIS for data analysis. To analyze two polygonal vector layers in QGIS and calculate the percentage of polygons from one layer relative to the polygons of the other layer, PyQGIS the Python API for QGIS was used.

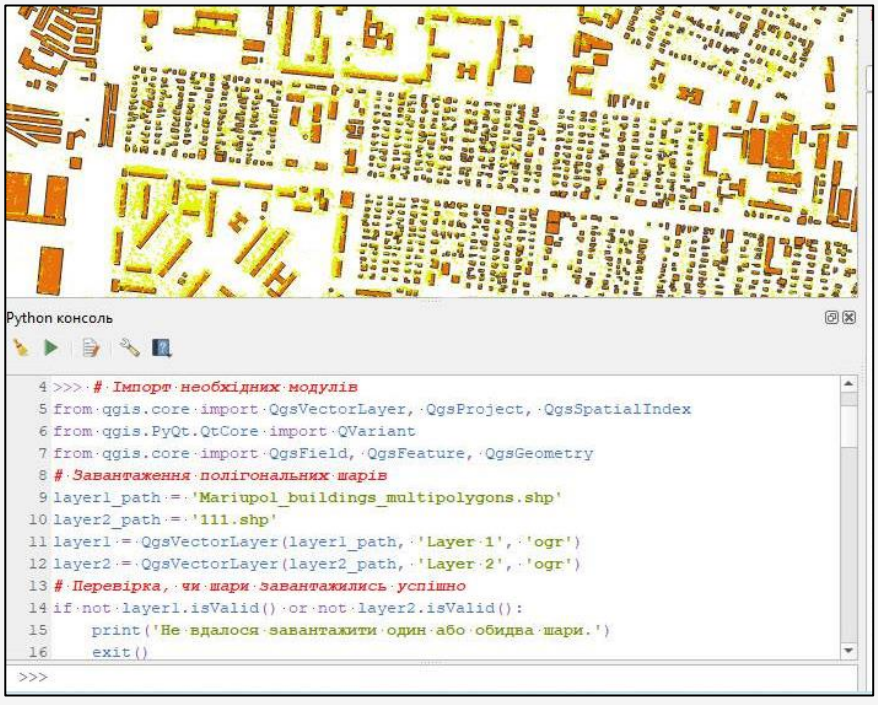


**Figure 9:** Execution of the script we wrote for analyzing two polygonal vector layers in QGIS and calculating the percentage of polygons from one layer relative to the polygons of the other layer

This code was executed in the QGIS Python Console. Figure 9 shows the execution of this code in QGIS. Additionally, in the fragment of the vector layers overlay, one can see what we mentioned earlier regarding the destroyed high-rise buildings, the elements of which are located next to the former building. The script performs the following actions: it loads two polygonal layers from shapefile files, verifies if the layers were successfully loaded, and adds them to the current QGIS project. It then creates a spatial index for the second layer to speed up the search, iterates through all polygons in the first layer to check for intersections with polygons in the second layer, counts how many polygons from the second layer are contained within each polygon of the first layer, calculates the percentage of intersecting polygons relative to the total number of polygons in the first layer, and finally outputs the analysis results. According to the OSM map before the full-scale invasion of the Russian Federation, there were 56,680 buildings within the city of Mariupol. During the full-scale invasion, according to the difference indicators from satellite images, 8,349 buildings were destroyed, of which 2,013 were high-rise buildings, and 934 of these were completely destroyed.

## 4. Results and Discussions

### *4.1 Detection of Building Destruction in Moshchun Village, Kyiv Region*

As a result of loading space images into the viewer of the DeltaCue module, a visual comparison of the images can be conducted, as they are spatially referenced within the viewer. When manipulations such as enlargement, reduction, or movement are performed on one image, the same actions are automatically applied to the other. The extent of destruction caused by the Russian occupation is clearly observable. Fragments of enlarged images before and after the occupation are presented in Figure 10. Since the satellite image dated 27/04/2020 was obtained in early 2022, there was a restriction on publishing high-resolution geospatial data over the territory of Ukraine due to security concerns, and the resolution of the image was intentionally reduced. As an experiment, we first implemented changes detection in space images using two groups of filters: spectral segmentation and misregistration of pixels of a pair of images. During implementation the spatial filtering was inactive. Seven iterations of image filtering were carried out. After that, at the 8th iteration the deterioration of results was already observed.

(a)

(b)

**Figure 10:** Enlarged fragments of space images of Moshchun village: (a) before the occupation, (b) after the occupation

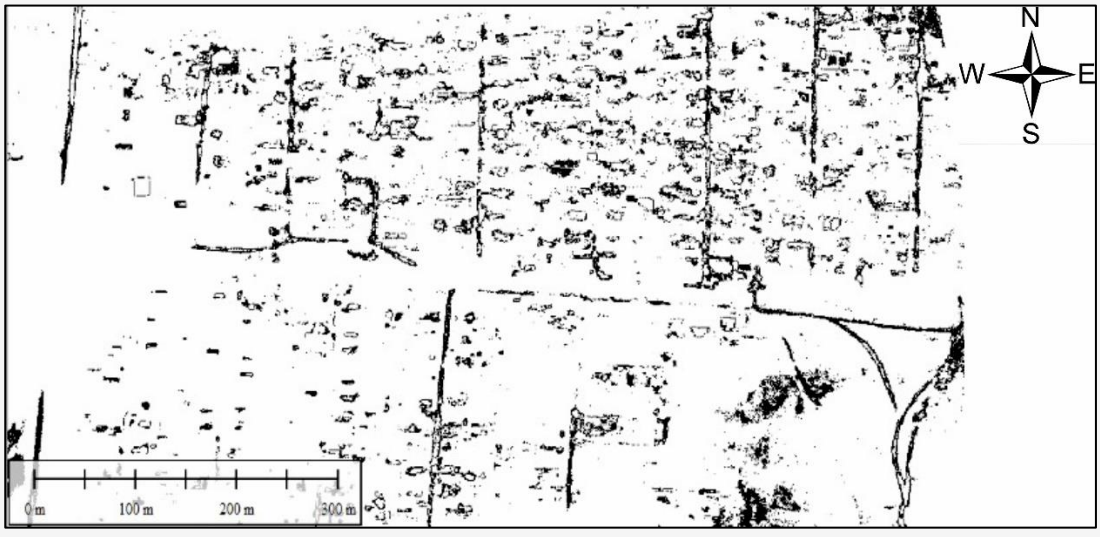


**Figure 11:** Unsatisfactory difference indicators of destruction were obtained after applying two groups of filters of space images

The resulting difference indicators contain a lot of noise, false data (roads, because the pictures were taken in different weather conditions), moving objects (cars, etc.), which give an unsatisfactory result (Figure 11). In the next stage, change detection was carried out by applying all filters, including a spatial filter that calculates several geometric properties based on the outline [36]. These properties include area, length of the main axis, length of minor axes, compactness, and elongation. For our study, the geometric properties used were area, compactness, and elongation.

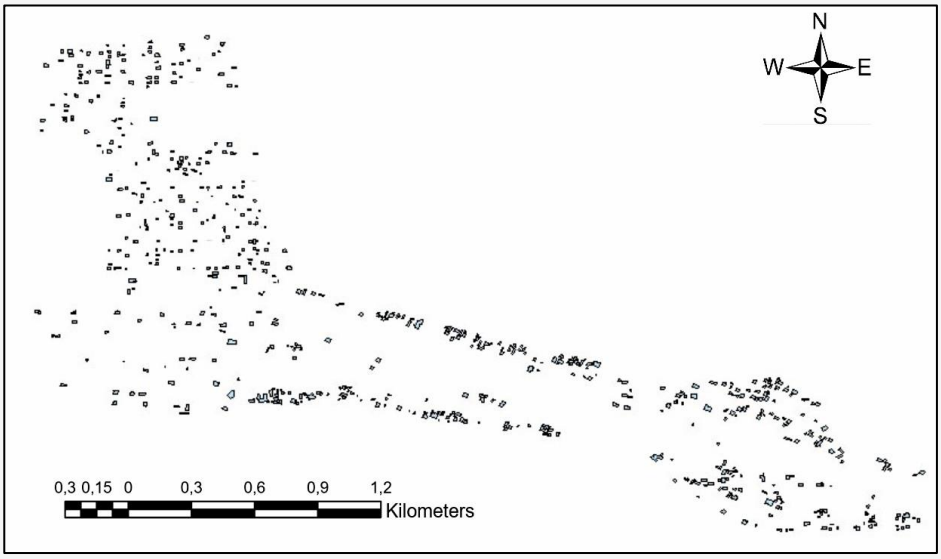


**Figure 12:** Vector layer of destroyed buildings in the village of Moshchun after the Russian occupation

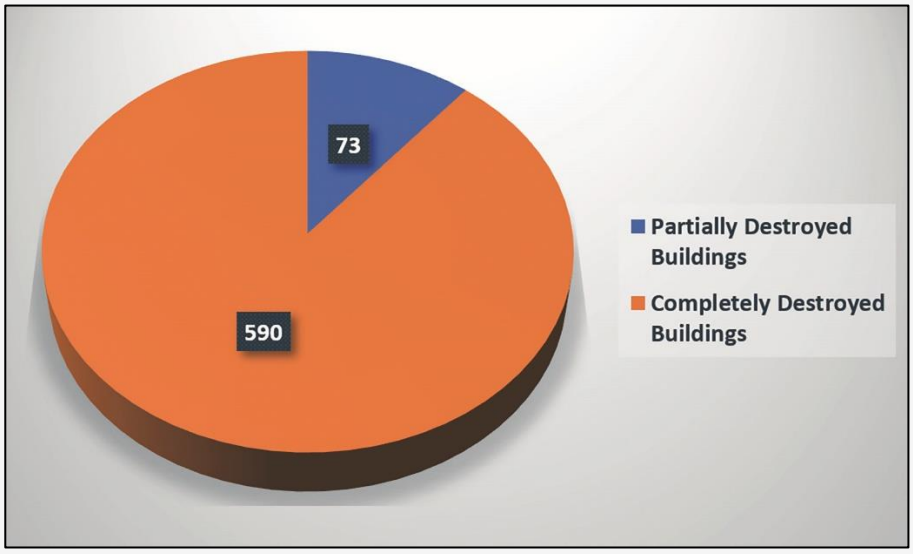


**Figure 13:** Diagram of the ratio of the degree of buildings destruction

As a result of using 6 iterations in the DeltaCue module, a vector layer with detected changes in multi-temporal images is created. The vector layer was refined manually. Needless erroneous data, objects of buildings that were built after 2020, moving objects (cars, etc.), foundations of buildings that were not built were removed. The determined total number of destroyed objects is 663 buildings (Figure 12). Of these, 590 buildings were completely destroyed up to the foundation or up to the walls, 73 buildings were partially damaged or partially destroyed. The total projected area of destroyed objects is 55449m$^2$ (Figure 13). Obtaining data compared to on-site inspection of the settlement after the territory's de-occupation. After calculation, a 100% match was found in the number of destroyed objects, with the only difference being in the analysis of the degree of destruction. During the on-site inspection of the settlement, 6 buildings that were considered 100% destroyed in the software calculation were found to be partially damaged and eligible for restoration. Verification of the accuracy of obtained data on building destruction is a key task that can be addressed through the use of temporally diverse satellite imagery and orthophotoplans acquired from unmanned aerial vehicles (UAVs) following the completion of combat operations.

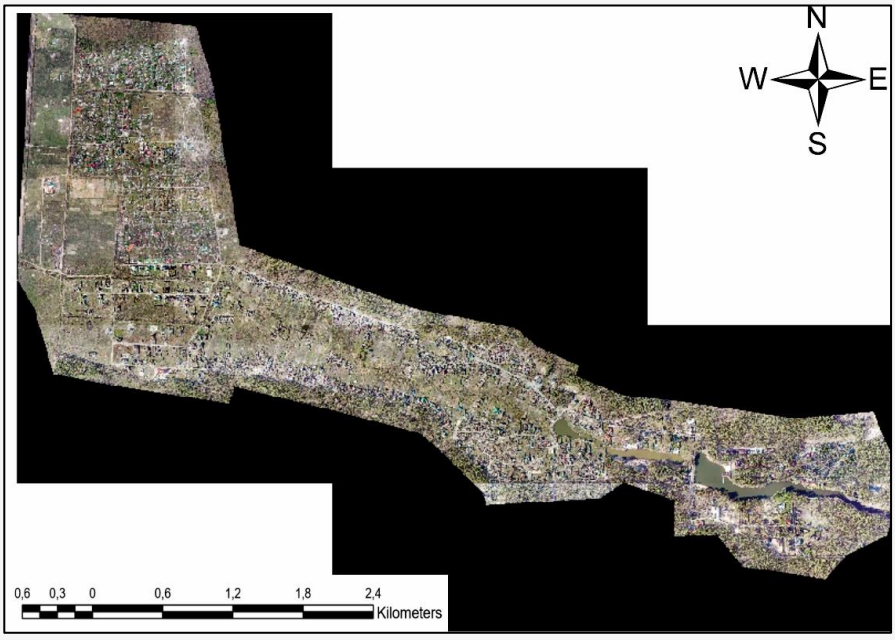


**Figure 14:** The orthophoto plan was constructed from aerial images obtained with the UAV DJI Phantom2RTK after the de-occupation of Moshchun

**Figure 15:** Enlarged fragments of the orthophoto plan showing the scale of destruction to civilian structures

Analysis of satellite images conducted at various time intervals after the cessation of hostilities provides the opportunity to detect and identify changes in the structure of buildings, their condition, and the extent of destruction. Orthophotoplans, generated using UAVs, enable the acquisition of high-quality geospatial images, facilitating precise analysis of objects and their condition. This method allows for the effective utilization of the acquired data in developing strategies for the restoration and reconstruction of damaged objects. Thus, the use of orthophotoplans obtained from UAVs after combat operations becomes a necessary and efficient tool for verifying the accuracy and analyzing the destruction of buildings. This approach is defined by the importance of timeliness and accuracy of the obtained data in the context of recovery and reconstruction efforts following conflicts and natural disasters. As a reference material, an orthophoto plan of the village Moshchun was utilized, constructed from aerial images obtained with the UAV DJI Phantom2RTK on July 14, 2022, after the de-occupation (Figure 14). The aerial survey was conducted at an altitude of 150 meters, resulting in 467 aerial images. The calculation of damaged buildings was carried out manually, zooming in on the orthophoto plan for maximum clarity in interpretation (Figure 15). The determined total number of destroyed objects from the orthophoto plan is 665 buildings, which is two destroyed buildings more than those automatically identified through satellite imagery.

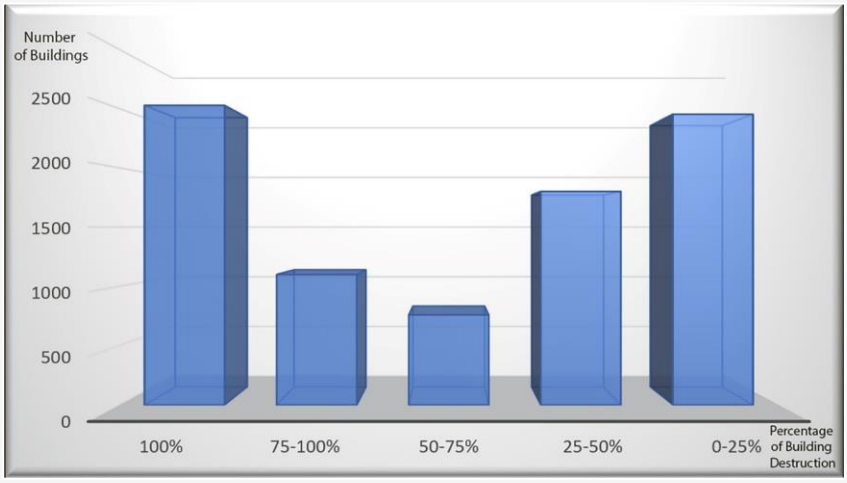


**Figure 16:** Building destructions in the city of Mariupol as a result of Russian aggression

This discrepancy is attributed to minor damages in two buildings that were not clearly interpreted due to the spatial resolution of the satellite images. Among them, 590 buildings were completely destroyed down to the foundation or walls, while 73 buildings were partially damaged or partially destroyed, aligning with a 99.70% match with the figures obtained in automatic mode.

*4.2 Detection of Building Destruction in Mariupol*

To determine the percentage of destruction, algorithms were used to compare classified destruction data stored in a vector file with the vector layer of buildings before the occupation and destruction of objects. Specifically, the area of destruction was compared to the total area of the object, and the percentage of destruction was calculated. Figure 16 shows the number of destroyed buildings in the city of Mariupol according to the proposed grading: buildings destroyed from 0 to 25 percent, buildings destroyed from 25 to 50 percent, buildings destroyed from 50 to 75 percent, buildings destroyed from 75 to 100 percent, and buildings completely destroyed.

**5. Recommendations**

Currently, in Ukraine, GIS and remote sensing experts are studying various methods of automatic or semi-automatic processing of aerial and space images with purpose of the fastest obtaining the resulting data on the damage to one or another settlement as a result of Russian aggression after their liberation from occupation. In addition, the smallest economic component of obtaining the necessary data is also taken into account. Experts process images using different methods in different software (ArcGIS, ENVI, QGIS, Erdas, etc.).

The method proposed in this paper, in our opinion, is one of the most effective, since the results are obtained by a semi-automatic method in a fairly short period of time (it took us 2 weeks to obtain the final results, including research works, applying different filtering capabilities). The method does not take into account the area of vertical damage, so it can be considered only preliminary for obtaining operational information about destructions, and not for calculating economic losses.

**6. Discussions**

Validation of the obtained results was conducted through a combination of independent data sources and ground-truth comparisons. In Moshchun, direct UAV imaging allowed for an on-site verification of the accuracy of detected damages, confirming that the satellite-based approach successfully captured large-scale destruction patterns. The alignment between UAV and satellite results supports the reliability of the proposed method in areas where UAV surveys are not feasible. In Mariupol, validation was conducted by cross-referencing destruction estimates with OpenStreetMap (OSM) data and pre-war building records. Given that physical access to Mariupol remains restricted due to the ongoing occupation, remote sensing remains the primary tool for assessing destruction. The use of OSM data facilitated an accurate estimation of pre-war structures, ensuring a reliable comparison between pre- and post-destruction building counts. The results were further corroborated by independent reports and publicly available geospatial data, confirming the large-scale destruction observed in satellite imagery. The findings of this study provide a critical contribution to the field of remote sensing for conflict damage assessment.

The demonstrated accuracy of multi-temporal satellite imagery analysis highlights the potential of automated change detection methods in large-scale urban damage assessments. The study's results align with previous research on post-conflict damage assessment, reinforcing the necessity of high-resolution imagery for accurate urban reconstruction planning.

Unexpected findings, such as minor discrepancies between UAV and satellite detection results, underscore the need for hybrid approaches that integrate multiple data sources. These variations highlight the limitations of satellite-based analysis for detecting subtle damage and emphasize the importance of incorporating UAV data where feasible. The broader implications of this research extend to humanitarian response, urban planning, and post-war reconstruction. By providing a systematic approach to quantifying destruction, the methodology can aid government agencies, non-governmental organizations, and international bodies in prioritizing recovery efforts. The ability to conduct remote damage assessments in inaccessible areas also demonstrates the practical value of this approach in conflict zones and disaster-stricken regions.

This study has significant practical and theoretical implications in the fields of remote sensing, urban planning, and post-conflict reconstruction. Practically, the proposed methodology enables efficient, large-scale damage assessment in war-affected areas, providing essential data for humanitarian organizations, government agencies, and urban planners engaged in reconstruction efforts. The ability to conduct accurate remote assessments without requiring on-site inspections is particularly valuable in conflict zones, where access is restricted. Theoretically, this research advances the field of geospatial analysis by demonstrating the effectiveness of multi-temporal satellite imagery combined with advanced change detection algorithms. It contributes to the ongoing development of automated damage assessment techniques, paving the way for future studies to refine and enhance remote sensing methodologies. Additionally, the findings underscore the importance of integrating different data sources, such as UAV imagery and OSM datasets, to improve accuracy and reliability. This research serves as a foundation for further exploration into AI-based classification techniques and hybrid approaches that leverage multiple remote sensing technologies for more comprehensive and precise destruction assessment.

## 7. Conclusion

The research has resulted in the development of a methodology for the rapid detection of destruction in Ukrainian settlements caused by Russian aggression, utilizing multi-temporal ultra-high-resolution satellite imagery. The proposed approach, based on the DeltaCue Remote Sensing module of Erdas Imagine, has demonstrated high efficiency in assessing large-scale damage, offering improved accuracy through its advanced object filtering techniques. By applying this methodology to analyze destruction in Moshchun and Mariupol, the study has confirmed the extensive impact of military actions on urban infrastructure. The findings underscore the significant role of remote sensing technologies in conflict damage assessment, providing a scalable and objective method for tracking destruction in inaccessible areas. The ability to differentiate between fully destroyed and partially damaged structures ensures a more precise evaluation of war-induced devastation, which is critical for post-conflict recovery planning.

Future research should focus on expanding the methodology to other affected regions, integrating AI-driven object recognition to enhance automation, and improving international cooperation for data validation. Additionally, the implementation of national programs for systematic satellite monitoring will be essential for guiding reconstruction efforts and humanitarian responses. This study contributes to the broader field of remote sensing applications in post-war recovery, reinforcing the necessity of technological advancements in urban damage assessment and reconstruction planning.

## References

[1] Poltavets, M. and Lakhtarenko, O., (2024). Technologies for Assessing the Operational Quality of Industrial Buildings as a Consequence of Partial Military Destruction. *Bridges and Tunnels: Theory, Research, Practice.* Vol. 25, 87-95. https://doi.org/10.15802/bttrp2024/303399.

[2] Azimi, M., Eslamlou, A. and Pekcan, G., (2020). Data-Driven Structural Health Monitoring and Damage Detection through Deep Learning: State-of-the-Art Review. *Sensors*, Vol. 20(10). https://doi.org/10.3390/s20102778.

[3] Xing, Z., Jianhao, B. and Yinghua, F., (2023). Change Detection Based on Tensor Robust Principal Component Analysis for Retinal Fundus Image Serial. *Information and Control*, Vol. 52, 115-128. https://doi.org/10.13976/j.cnki.xk.2023.2131.

[4] Chetverikov, B., Trevoho, I., Prokhorchuk, O., Vladimirov, S. and Herasymchuk, P., (2024). Synergy of UAV Aerial Survey Methods and LiDAR Scanning for the Study of Planar Objects of Historical and Cultural Heritage. *International Journal of Geoinformatics*, Vol. 20(9), 98–111. https://doi.org/10.52939/ijg.v20i9.3551.

[5] Chetverikov, B., Różycki, S., Malitskyi, A. and Babiy, L., (2024). Application of Orthophoto Maps Created from UAV Aerial Images for Monitoring Historical and Cultural Heritage Lands. *Journal of Environmental & Earth Sciences*. Vol. 6(2), 144–163. https://doi.org/10.30564/jees.v6i2.6360.

[6] Chetverikov, B., Trevoho, I., Babiy, L., Marusazh, K. and Abdallah, R., (2020). Determination of Quantitative Indicators of Earthquake Destruction by Different Time Space Images [Electronic resource]. *GeoTerrace-2020: International scientific and technical conference of young professionals*, December 7-9, Lviv. https://eage.in.ua/wp-content/uploads/2020/12/GeoTerrace-2020-065.pdf.

[7] Dorozhynskyy, O., Chetverikov, B. and Babiy, L., (2013). Determining the Influence of Earthquake on the Changes of Objects Using Remote Sensing Data. *Geomatics, Land management and Landscape*, Vol. 3, 7–15. https://doi.org/10.15576/GLL/2013.3.7.

[8] Demin, A., Sechak, E. and Prisyazhnyuk, S., (2021). Determining the Composition of an Object Based on its Hyperspectral Image. *Computer Optics*, Vol. 45(3), 394-398. https://doi.org/10.18287/2412-6179-CO-697.

[9] Lindquist, E. and D'Annunzio, R., (2016). Assessing Global Forest Land-Use Change by Object-Based Image Analysis. *Remote Sensing*, Vol. 8. https://doi.org/10.3390/rs8080678.

[10] Alsabhan, W., Alotaiby, T. and Dudin, B., (2022) Detecting Buildings and Nonbuildings from Satellite Images Using U-Net. *Hindawi Computational Intelligence and Neuroscience*, Vol. 13. https://doi.org/10.1155/2022/4831223.

[11] Delibasoglu, I. and Cetin, M., (2020). Improved U-Nets with Inception Blocks for Building Detection, *Journal of Applied Remote Sensing*, Vol. 14(04). https://doi.org/10.1117/1.JRS.14.044512.

[12] Ghanea, M., Moallem, P. and Momeni, M., (2016). Building Extraction from High-Resolution Satellite Images in Urban Areas: Recent Methods and Strategies Against Significant Challenges, *International Journal of Remote Sensing*, Vol. 37(21), 5234-5248. https://doi.org/10.1080/01431161.2016.1230287.

[13] Huang, X. and Zhang L., (2012). Morphological Building/Shadow Index for Building Extraction from High-Resolution Imagery Over Urban Areas, *IEEE Journal of Selected Topics in Applied Earth Observations and Remote Sensing*, Vol. 5(1), 161–172. https://doi.org/10.1109/JSTARS.2011.2168195.

[14] Saito, S., Yamashita, T. and Aoki, Y., (2016). Multiple Object Extraction from Aerial Imagery with Convolutional Neural Networks, *Electronic Imaging*, Vol. 28(10), 1–9. https://doi.org/10.2352/ISSN.2470-1173.2016.10.ROBVIS-392.

[15] Yuan. J., (2018). Learning Building Extraction in Aerial Scenes with Convolutional Networks, *IEEE Transactions on Pattern Analysis and Machine Intelligence*, Vol. 40(11), 2793–2798. https://doi.org/10.1109/TPAMI.2017.2750680.

[16] Wang, J., Yang, X., Qin, X., Ye, X. and Qin, Q., (2014). An Efficient Approach for Automatic Rectangular Building Extraction from Very High Resolution Optical Satellite Imagery, *IEEE Geoscience and Remote Sensing Letters*, Vol. 12(3), 487–491. https://doi.org/10.1109/LGRS.2014.2347332.

[17] Guo, Z., Shao, X., Xu, Y., Miyazaki, H., Ohira, W. and Shibasaki, R., (2016). Identification of Village Building Via Google Earth Images and Supervised Machine Learning Methods, *Remote Sensing*, Vol. 8(4), 271. https://doi.org/10.3390/rs8040271.

[18] Vakalopoulou, M., Karantzalos, K., Komodakis, N. and Paragios, N., (2015). Building Detection in Very High Resolution Multispectral Data with Deep Learning Features, *IEEE International Geoscience and Remote Sensing Symposium (IGARSS*), 1873–1876, Milan, Italy, July 2015. https://doi.org/10.1109/IGARSS.2015.7326158.

[19] Kholoshyn, I., Syvyj, M., Mantulenko, S., Shevchenko, O., Sherick, D. and Mantulenko, K., (2023). Assessment of Military Destruction in Ukraine and its Consequences Using Remote Sensing. *IOP Conference Series: Earth and Environmental Science*, Vol. 1254. https://doi.org/10.1088/1755-1315/1254/1/012132.

[20] Sirmacek, B. and Unsalan, C., (2011). A Probabilistic Framework to Detect Buildings in Aerial and Satellite Images, *IEEE Transactions on Geoscience and Remote Sensing*, Vol. 49(1), 211–221. https://doi.org/10.1109/TGRS.2010.2053713.

[21] Gong, J., Sui, H., Ma, G. and Zhou, Q., (2008). Review of Multi-Temporal Remote Sensing Data Change Detection Algorithms *the International Archives of the Photogrammetry, Remote Sensing and Spatial Information Sciences.* Vol. XXXVII Part B., 757-762.

[22] Mueller, H., Groeger, A., Hersh, J., Matranga, A. and Serrat, J., (2021). Monitoring War Destruction from Space Using Machine Learning. *Proceedings of the National Academy of Sciences*. Vol. 118(23), 1-9. https://doi.org/10.1073/pnas.2025400118.

[23] Kaplan, G., Rashid, T., Gasparovic, M., Pietrelli, A. and Ferrara, V., (2022). Monitoring War-Generated Environmental Security Using Remote Sensing: A Review. *Land Degradation & Development*, Vol. 33(10), 1513–1526. https://doi.org/10.1002/ldr.4249.

[24] Kumar, S., Wickramasooriya, A. and Dilini, S., (2022). Analysis of Ammonium Nitrate Detonation Destruction in Beirut City Using Geospatial Techniques. *Spatial Information Research*, Vol. 30, 749–757. https://doi.org/10.1007/s41324-022-00459-0.

[25] Wang, N., Ruozhen, C., Chen, J., and Zhang, M. (2024). Streamlining BIM Models for GIS Integration: An Advanced Approach to Building Envelope Extraction. *International Journal of Digital Earth*, Vol. 17(1). https://doi.org/10.1080/17538947.2024.2368708.

[26] Yavorska, O. and Barabanov, S., (2024). Identification of Hidden Damage in Constructive Elements of Buildings and Structures to Reduce the Risks of their Destruction. *Ukrainian Journal of Civil Engineering and Architecture*, Vol. 2(020), 116-125. https://doi.org/10.30838/J.BPSACEA.2312.260324.116.1050.

[27] Zhang, W. and Jiang, Y., (2023). GIS Building Reconstruction Research Based on 3D Image Processing Technology, 1116-1123. https://doi.org/10.3233/ATDE231054.

[28] Huangfu, D., Rong, L. and Wei, G., (2023). Application of High-Rise Building Fire Rescue Based on BIM and GIS. *Proceedings of the 27th International Symposium on Advancement of Construction Management and Real Estate*, 74-84. https://doi.org/10.1007/978-981-99-3626-7_6.

[29] Law, S., Seresinhe, C., Shen, Y. and Gutierrez-Roig, M., (2020). Street-Frontage-Net: Urban Image Classification Using Deep Convolutional Neural Networks. *International Journal of Geographical Information Science*, Vol. 34, 681-707. https://doi.org/10.1080/13658816.2018.1555832.

[30] Maltseva, I., Meng, T., Xiao, S., Yizhi, C. and Zeng, L., (2024). An Integrated Review and Analysis of Urban Building Seismic Disaster Management Based on BIM-GIS. *E3S Web of Conferences*, Vol. 474(4). https://doi.org/10.1051/e3sconf/202447402013.

[31] Rai, V., Singh, S., Tekam, Y., Upadhyay, S. and Sahu, D., (2023). Enhancing Soil Degradation Assessment through the Integration of GIS and RS: A Comprehensive Review. *International Journal of Environment and Climate Change*, Vol. 13, 2622-2632. https://doi.org/10.9734/ijecc/2023/v13i92559.

[32] Shalaby, A. and Tateishi, R., (2007). Remote Sensing and GIS for Mapping and Monitoring Land Cover and Land-Use Changes in the Northwestern Coastal Zone of Egypt. *Applied Geography*, Vol. 27, 28-41. https://doi.org/10.1016/j.apgeog.2006.09.004.

[33] Shi, J., (2024). Construction and Application of Three-Dimensional Information Management System for Intelligent Buildings Integrating BIM and GIS Technologies. *Scalable Computing: Practice and Experience*, Vol. 25, 2985-3000. https://doi.org/10.12694/scpe.v25i4.2939.

[34] Sun Y. and Li X. (2010). Data Fusion of GIS and RS by Neural Network. *International Conference on Intelligent Control and Information Processing*, Dalian, China, 648-651. https://doi.org/10.1109/ICICIP.2010.5564216.

[35] Marmanis, D., Wegner, J. D., Galliani, S., Schindler, K., Datcu, M. and Stilla, U., (2016). Semantic Segmentation of Aerial Images with an Ensemble of CNNs, *ISPRS Annals of the Photogrammetry Remote Sensing and Spatial Information Sciences*, Vol. III-3, 12–19 July 2016. https://doi.org/10.5194/isprs-annals-III-3-473-2016, 2016.

[36] Yang, H. X., Wang, X. Q., Dou, A. X. and Li, Z. M., (2015). Multi-Source and Multi-Factor Gridding Method of Building Distribution Based on RS and GIS. *Earthquake*, Vol. 35, 136-146. https://dizhen.ief.ac.cn/EN/Y2015/V35/I3/136.